Journal of Structural Engineering and Geotechnics,
13(1), 37-48, Winter & Spring 2023

Multi-Objective Optimization of the Depth and Cementation of Liquefiable Soil Surrounding Tunnels

Mohammad Shabani SoltanMoradi [a], Mohammad Azadi [a,*], Homayoun Jahanian [a]

[a] *Department of Civil Engineering, Qazvin Branch, Islamic Azad University, Qazvin, Iran*
Received 23 December 2024, Accepted 28 May 2024

Abstract

Designing tunnels in liquefiable sandy soils presents a significant challenge in determining the optimal depth and extent of the soil cementation around them. Reducing the depth of the tunnel decreases both the bending anchor force and the axial load on the tunnel's shell, yet it leads to an increase in ground surface settlement, and the opposite is true when depth is increased. Enhancing the cementation level at the tunnel's optimal depth reduces both structural uplift and shear forces exerted on the tunnel lining. Still, it also leads to an increase in axial loads and vice versa. Given the contradictory nature of these outcomes, the FLAC software was employed to simulate tunnels in liquefiable soils to address this dilemma. Subsequently, a neural network was utilized to identify the correlations between the inputs and outputs of the simulation. This network was the objective function for identifying optimal values by applying a genetic algorithm. Optimal design parameters were derived using the NSGA-II modified algorithm, a multi-objective optimization technique based on the objective functions. Ultimately, Pareto charts generated from the multi-objective optimization process enabled designers to select the most suitable tunnel location according to their specific requirements concerning depth and the soil cementation in liquefied soils.

Keywords: Multi-Objective Optimization, Liquefaction, Pore Water Pressure, Neural Network, Uplift

1.Introduction

The excess pore water pressure generated in saturated sandy soil during an earthquake reduces the effective soil stress and resistance, ultimately resulting in soil liquefaction. Excavating tunnels near the earth's surface can also reduce soil resistance and cause the uplift of both the structure and earth's surface[1]. In a study by Liu and Song, the effects of liquefaction on underground structures were investigated, and it was reported that soil liquefaction results in the uplift of the structure (Fig. 1). They also stated that the uplift of the structure and ground surface heave were 36 and 34 cm, respectively[2].

Ji-Lei Hu et al. (2017) used the FE-FD method to design underground structures. They also investigated the behavior of underground structures by applying seismic force to a subway station at different depths. They reported that as the seismic load time increases, the degree of liquefaction of the surrounding soils and the uplift behavior of the underground structure increases [3].

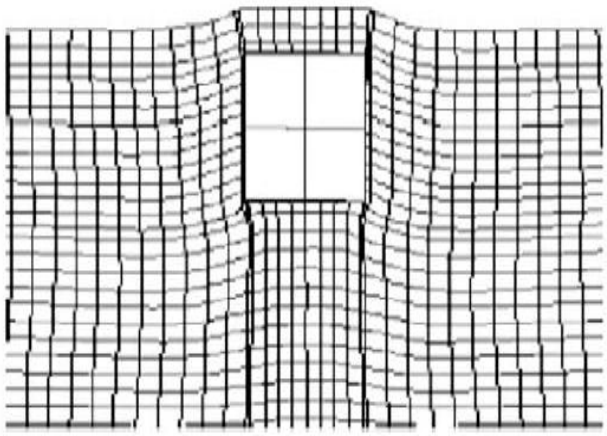

Fig 1. Display of structure and surface ground uplift due to the dynamic loading (2)

Gang et al. (2020) used artificial neural network (ANN) and support vector machine (SVM) models to predict the liquefaction-induced uplift displacement of underground structures [4].Qing Liao et al. (2019) investigated various parameters of tunnels exposed to liquefaction using multi-objective optimization. They reported that two contradictory objectives can be

*Corresponding Author: Email Address: azadi@qiau.ac.ir

simultaneously optimized using a multi-objective optimization method [5]. Nokande et al. (2023) used the shaking table test to minimize the liquefaction-induced uplift of tunnels excavated near the Earth's surface. They reported that helical piles can significantly decrease rapid tunnel uplift in this soil type [6]. Rashiddel et al. (2024) studied the impact of psychopathy on the soil surrounding shallow tunnels and the interaction between the tunnel and the superstructure[7]. ZHONG et al. (2024) used SPT testing to investigate the uplift values of tunnels excavated in cohesive soils. The results show that the more minor SPT-blow counts and tunnel depth are, the larger the uplift is [8]. Azadi et al. (2010) investigated pore water pressure and effective stress at the top and bottom of the tunnel. They reported that structural uplifting-induced swell of the ground gradually decreases with increasing distance from the location of the tunnel [9].

The Cementation (bonding between the grains) is one of the effective factors in reducing the liquefaction potential. Therefore, it is possible to increase the resistance of non-cemented soils against liquefaction using artificial cementation. Azadi et al. (2007) investigated the axial force and sheer force of the tunnel lining by increasing the cementation degree. They stated that as the degree of the cementation of the soil surrounding the tunnel increases, the axial force increases and the shear force decreases. They also assessed the uplift of the Earth's surface. The results showed that as the degree of the cementation of the soil surrounding the tunnel increases, the uplift of the Earth's surface decreases significantly [10]. Wayne et al. (1989) performed several laboratory tests on the liquefaction of sands. They indicated that the percentage of clay particles is one of the main factors affecting the liquefaction behavior of soils [11].

Liang et al. (2000) conducted dynamic triaxial laboratory tests on damaged samples to investigate the effects of clay particles on the liquefaction behavior of soils. The tests were performed on eight soil groups, including 65 samples with different clay particles [12]. Furthermore, several shaking table tests were conducted to obtain the forces and anchors acting on the tunnel lining in liquefiable soils [13]

Artificial intelligence methods used to solve geotechnical engineering problems can also be used to find the relationship between the input and output parameters of the objective function. So far, very few studies have been performed in the field of multi-objective optimization of NSGA II to assess the tunnel depth and the cementation degree of the soil surrounding the tunnel in a liquefaction-prone zone. In most studies, the optimization has been performed as a single objective, with few evaluating conflicting results simultaneously. These cases indicate the difference between the present study and previous studies and are supposed one of the strengths of this study. Therefore, the present study aims to investigate the depth of the tunnel, the uplift of the Earth's surface, the forces and moment acting on the tunnel lining, and the degree of the cementation of the soil surrounding the tunnel at the optimum depth and optimize the results using the multi-objective genetic algorithm.

2. Methodology

Generally, there is no specific analytical or numerical method for designing and determining the depth of the tunnel and the degree of the cementation of the soil surrounding the tunnels in the form of multi-objective optimization. Most studies have used single-objective optimization methods, and simultaneous optimization of various parameters has not been conducted. Therefore, this study employed multi-objective optimization methods.

In this method, several objective functions are defined, and then optimized simultaneously. In most cases, the defined objective functions conflict, where improvement in one objective function leads to a decline in the other objective functions. Therefore, there is no unique solution that optimizes all the defined objective functions simultaneously. A set of optimal solutions called Pareto curves [14] can be used to perform multi-objective optimization simultaneously. NSGA-II is one of the best multi-objective optimization algorithms introduced by Deb, which performs faster and better in finding a set of non-superior solutions [15]. In this study, the modified NSGA-II algorithm [16] was used for multi-objective optimization of the tunnel depth and the cementation degree of the liquefiable soil surrounding the tunnel at the optimum depth. This method is expected to obtain the optimum depth of the tunnel and the optimum degree of the cementation of the liquefiable soil surrounding the tunnel based on the bending moment and axial force acting on the tunnel lining and the uplift rate of earth's surface simultaneously. As a result, the modified NSGA-II algorithm provided all the optimal points of the design in terms of the objective functions.

3. Concepts in Multi-Objective Optimization

In multi-objective optimization problems, the goal is looking to find the design vector $X^* = [x_1^*. x_2^*. \dots . x_n^*]$, a member of R^n, which can optimize the target function $F = [f_1(x). f_2(x). \dots . f_k(x)]^T$, a member of R^k, under m, the unequal condition as per equation 1 and P, the equal condition, as per equation 2.

$$g_t(x) \leq 0 \qquad t = 1.2. \dots . m \tag{1}$$

$$h_j(x) = 0 \qquad j = 1.2. \dots . p \tag{2}$$

Regardless of the reduction in the generality of the problems, if we aim to minimize all objective function vectors, multi-objective optimization is categorized as Pareto problems [14]and is introduced as follows.

3.1. Pareto dominated

Vector $U = [u_1. u_2. \dots . u_n]$ has Pareto dominance over vector $V = [v_1. v_2. \dots . v_n]$, $(U < V)$ if and only if the following expression stands:

$$\forall i \in \{1.2. \dots . \mathrm{k}\}. u_i \leq v_i \wedge \exists_j \in \{1. 2. \dots . k\}: u_i < v_j \tag{3}$$

3.2. Pareto Optimality

A point $X^* \in \Omega$ (Ω is an acceptable design area that can satisfy Equations 1 and 2) is called a Pareto optimal point if no other point in Ω dominates it. If and only if $F(X^*) < F(X)$. this can be described as the following:

$$\forall X \in \Omega. X \neq X^*. \exists_i \in \{1.2. \dots . k\} : f_i(X^*) < f_i(X) \tag{4}$$

(4)

3.3. Pareto Set

In multi-objective optimization problems, a Pareto set (P^*) includes all Pareto optimal vectors.

$$P^* = \{X \in \Omega | \exists X' \in \Omega: F(X') < F(X)\} \tag{5}$$

Conventional methods rely on derivatives of the function for optimization, whereas evolutionary algorithms do not require derivatives of the function and only utilize the function's value itself. While other iterative methods start from an initial point to find a solution and only return a single answer in each run, evolutionary algorithms divide the search space into several subsections and employ various initial points to decrease the likelihood of becoming trapped in local optimal points. These algorithms can obtain various points from the set of optimal problem points in just one run.

4. Numerical analysis

4.1. Geometry of the model and the conditions created in the software

Figure 2 illustrates the dimensions of the model, tunnel size, and meshing method used. The modeling dimensions were selected in a manner that places the bedrock at the bottom of the model, with a depth of 30 meters from the ground surface. To ensure that the results obtained are not affected by lateral boundaries, the width of the model on both sides was supposed to be more than 5 times the diameter of the tunnel, including the tunnel itself. As a result, the percentage of error caused by stresses in the modeling results was reduced to 5%, and the effect of boundaries on the analyses could be disregarded.

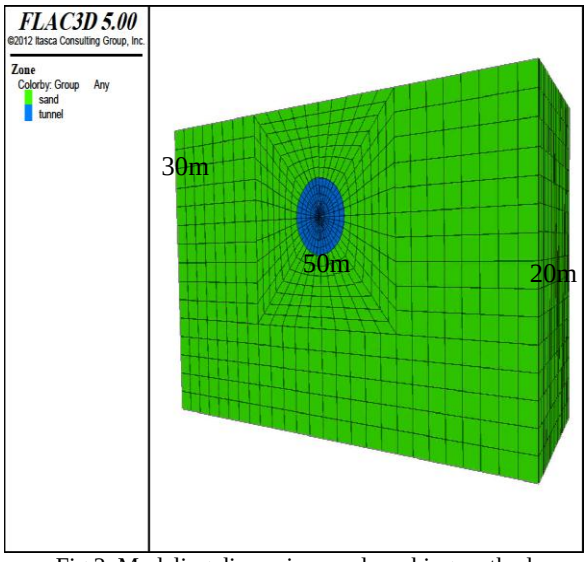

Fig 2. Modeling dimensions and meshing method

The dimensions and size of the mesh used in the modeling should be small enough to allow for the propagation of shear waves. Lysmer and Kuhlemeyer have reported that the accuracy of wave propagation in numerical modeling is determined by the wavelength. The size of the wavelength, in turn, depends on the dimensions of the elements in the direction of wave propagation. It is necessary that the dimensions of the elements are smaller than $\frac{1}{8}$ to $\frac{1}{10}$ of the wavelength. All input stimulus frequencies utilized in the analysis were supposed to be above 25 Hz [17]. To assess the liquefaction conditions, the soil must be completely saturated. Thus, the level of the underground water was supposed as the ground level.

4.2. Soil Specifications

Table 1 shows the parameters related to liquefiable sandy soil. The characteristics of liquefiable sandy soil were selected based on studies by Khoshnoudian and Shahrour [18], Liu and Song [2], Azadi and Hosseini [1], Shabani and Azadi [19], and the VELACS project [20] in the state of Nevada, USA.

Table 1
Behavioral Model and Soil Specifications

Soil type	Behavioral model	Shear modulus (MPa)	Bulk modulus (MPa)	φ (^{0})	C (kPa)	γ_d (kN/m^3)	K (m/sec)
Sand soil	Finn	20	30	25	0	15	10^{-4}

The selected sandy soil was loose and liquefied under dynamic loading. Therefore, the effect of liquefaction of these soils on the tunnel lining and surrounding soil under different conditions and dynamic loading was assessed. To assess the effect of liquefaction on multi-objective optimization, the soil behavior modeling in FLAC software should be selected in a way that considers the increase in permeability pressure, the decrease in effective stress, and the volume changes of soil under dynamic loads during liquefaction. Therefore, Finn's behavioral model, which models soil liquefaction based on changes in strain rate, was used. This model, presented by Martin et al. (1975), describes the relationship between changes in volumetric strain ($\Delta\varepsilon_{vd}$) and cyclic shear strain amplitude (γ) according to equation (6)[21]:

$$\Delta\varepsilon_{vd} = C_1(\gamma - C_2\varepsilon_{vd}) + \frac{C_3\varepsilon_{vd}^2}{\gamma + C_4\varepsilon_{vd}} \quad (6)$$

C1 through C4 are coefficients which are obtained from cyclical triaxial experiments. These coefficients were set to 0.76, 0.52, 0.2 and 0.5 respectively, based on the study by Pashangpishe [20].

4.3. Dynamic Loading Conditions and Methods

Dynamic loading is a significant factor in creating liquefaction in sandy soils. The magnitude and characteristics of dynamic loading depend on various factors such as the type of load, damping, type of dynamic boundaries, duration of dynamic load, loading range, and frequency characteristics. To apply the load, a sinusoidal shear wave was supposed from the bedrock towards the ground surface according to equation (7).

$$\ddot{u}_g = A_g \sin(2\pi f t) \quad (7)$$

The study of Khoshnoudian [18] was used as a reference for selecting the loading range and the load duration, which were supposed to be 0.1 g and 10 seconds, respectively. Additionally, the input frequency and damping rate were supposed to be 1 Hz and 5%, respectively. Free field conditions were used to design absorbent boundaries and prevent the reflection of waves in the model. The shear wave, selected based on the characteristics of the case study, soil type, and bedrock condition, was used in the analysis after modification.

4.4. Characteristics of Tunnel Lining

Figure 3 illustrates the method of modeling and the location of the tunnel in FLAC software. Based on the figure, a tunnel with an external diameter of 6.9 meters, an elasticity modulus of E=2.236×10^7 kN/m^2, and a tunnel lining thickness of 30 cm was chosen. These parameters were extracted from a case study conducted in the Isfahan-Iran metro.

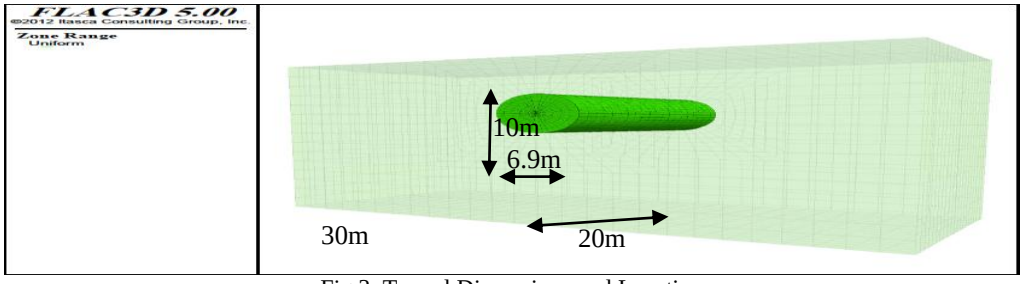

Fig 3. Tunnel Dimensions and Location

50m 20m

5. Model Validation

The results of the present study were compared and validated with the results of the centrifuge test and numerical modeling. In the centrifuge test conducted by Chain et al. [22], the diameter of the tunnel was 5 meters, and the buried depth was 7.5 meters. The modulus of elasticity and the thickness of the tunnel lining were $E=3 \times 10^7$ kN/m^2 and 0.35 meters, respectively. A sinusoidal wave was applied in the model, and the frequency, peak acceleration, and duration of the wave were chosen to be 0.75 Hz, 0.1 g, and 10 seconds, respectively. It was reported that the uplift of the ground surface after the liquefaction of the soil in the centrifuge test was about 100mm. Additionally, Azadi et al. [9] reported that the amount of axial force and bending moment on the tunnel lining was 54.3 (ton) and 11 (ton-m) at a depth of 8 meters, respectively.

In the present study, it was found that the uplift of the ground surface at a depth of 8 meters was equal to 88 mm, and the amount of axial force and bending moment on the tunnel lining was equal to 55.1 (ton) and 10.96 (ton-m), respectively. The results of the present study were found to be similar to those of other studies.

6. Evaluation of the Inputs and Outputs of Modeling in Optimization

6.1. Evaluation of the Depth of the Tunnel

As the depth of underground structures increases, their safety also increases [2]. However, as the depth of the tunnel increases, the amount of bending moment and axial force on the tunnel lining increases due to the increase in overhead on the tunnel crown. On the other hand, as the depth of the tunnel decreases, the uplift rate of the ground surface increases due to the liquefaction effects. Therefore, determining the depth of the tunnel is essential in reducing the amount of force applied to the tunnel lining and the uplift of the ground surface. To achieve this, a method that can optimize the conflicting results obtained from the depth is necessary. For this reason, NSGA-II multi-objective optimization was used to optimize the results simultaneously.

6.2 Evaluation of the Soil Cementation Around Tunnels

Soil cementation is an effective parameter in reducing the effects of liquefaction. It is one of the methods used for strengthening and has a significant impact on the uplift of the ground surface, as well as the forces and moments applied to the tunnel lining. As the soil cementation around the tunnels increases, the axial force on the tunnel lining also increases. Conversely, if the cementation of the soil surrounding the tunnels decreases, the uplift rate of the ground surface and the amount of shearing force on the tunnel lining increase. Given these considerations, it becomes crucial to determine the optimal level of the soil cementation around tunnels, especially when the results obtained conflict or not aligned with each other. Therefore, NSGA-II multi-objective optimization was used for this purpose.

7. Neural Network

The objective of the present study is to determine the optimal depth of a tunnel in liquefiable soils within the minimum and maximum values, considering specific dimensions and geotechnical parameters. Another aim is to determine the optimal amount of the soil cementation surrounding the tunnel at the optimal depth. This factor requires significant modeling, which cannot be achieved using FLAC or any other software.

The purpose of this study is not only to determine a value that meets geotechnical design parameters, but also to identify the optimal depth and the cementation of the soil surrounding the tunnel. Therefore, various models were created using a neural network. MATLAB software was used to process the data in matrix form consisting of numbers. The number of hidden layers in the network and the number of internal neurons in each layer are significant factors affecting the accuracy of the neural network. A feedforward neural network was trained using different objective functions, and different layers in the neural network program were trained based on the input and output data in the software [23]. In the present study, a neural network program with two layers and six hidden neurons was used for training and learning the relationship between the inputs and outputs of FLAC software.

7.1. Input and Output Vectors for Tunnel Depth and the Soil Cementation Rate in the Neural Network

The tunnel was modeled at different depths using FLAC software, and each model was subjected to a dynamic force Table 2. The tunnel depth (x1) was

chosen as the input for the neural network. The range of tunnel depth supposed was between 8 and 20 meters. Depths lower or higher than this range were not selected due to the lack of implementation and reduced liquefaction effects, respectively. The rest of the specifications and parameters related to the design were supposed fixed. Based on the analysis of the models, three outputs in the FLAC software, including the maximum bending moment (f1), the maximum axial force (f2) applied to the tunnel lining, and the uplift of the ground surface (f3), were selected as objective functions in the neural network. To train the neural network, the input and output vectors were randomly arranged. This approach prevented the neural network from memorizing them and instead allowed it to learn and adapt to them.

Table 2
The input and output vectors of the objective function in the neural network program

Number	**Neural Network Input**	**Target function in the Neural Network**		
	Tunnel depth (x1)(m)	**Maximum bending moment (f1) (ton-m)**	**Maximum axial force (f2) (ton)**	**ground level uplifting (f3) (mm)**
1	8.5	11.02	59.1	76
2	12.5	14.51	94.5	30.97
3	11	12.46	81.9	41.57
4	13.5	15.62	100.45	25.42
5	9	11.04	63.9	66
6	15	17.03	106.08	19.16
7	17	20.22	117.82	13.3
8	18.5	22.08	124.65	10.85
9	16	18.56	111.46	15.65
10	20	25.5	127.2	10
11	14	16.04	102	22.92
12	9.5	11.08	68.7	57
13	8	10.96	55.1	88
14	19	23.7	125.1	10.45
15	17.5	21.05	121	12.3
16	11.5	13.15	86.1	37.14
17	10	11.3	74.1	50
18	13	15.26	99.1	28.14
19	15.5	17.73	108.28	17.3
20	18	21.7	123.4	11.45
21	10.5	11.78	77.7	45
22	14.5	16.46	103.55	20.9
23	12	13.83	90.3	33.93
24	16.5	19.39	114.64	14.41
25	19.5	24.6	125.55	10.2

Different models of the cementation of soil surrounding the tunnels were performed in FLAC software Table 3. The cementation rate was selected as the input (x2) for the neural network program. The

depth of the tunnel was fixed at 12 meters in this modeling. The design range for the input part (x2) was selected between 0 and 30 kPa. Intervals outside this range were not supposed due to the lack of implementation in underground structures. Three outputs, including the maximum shear force (f1), the uplift of the ground surface (f2), and the maximum axial force on the tunnel lining (f3) were selected as objective functions in the neural network.

Table 3
The input and output vectors the cementation rate of the soil surrounding the tunnels in the neural network

Number	**Neural Network input**	**Target function in the Neural Network**		
	Cementation (x2) (kPa)	**maximum shear force (f1)(ton)**	**ground level uplifting (f2)(mm)**	**Maximum axial force (f3) (ton)**
1	11	9.14	9.16	76.57
2	20	5.7	5.02	77
3	28	4.61	2.98	77.65
4	8	9.56	12.3	76.2
5	30	4.48	2.57	77.8
6	15	7.56	6.76	76.79
7	6	9.73	15	75.65
8	24	5.01	3.92	77.27
9	3	9.91	19.82	74.55
10	0	10	12.3	76.2
11	18	6.23	5.64	76.94
12	26	4.78	3.43	77.44
13	13	8.54	7.79	76.69
14	1	9.98	23.5	73.58
15	29	4.54	2.77	77.73
16	9	9.46	11.1	76.38
17	16	7.02	6.34	76.84
18	22	5.31	4.45	77.15
19	4	9.86	18.11	74.95
20	27	4.69	3.2	77.58
21	25	4.89	3.67	77.36
22	5	9.8	16.51	75.3
23	2	9.95	21.6	74.1
24	19	5.93	5.32	76.7
25	7	9.65	13.61	75.95
26	23	5.15	4.18	77.2
27	10	9.32	10	76.5
28	17	6.58	5.97	76.87
29	12	8.89	8.42	76.63
30	21	5.49	4.73	77.07
31	14	8.12	7.24	76.74

7.2. Error Rate of the Neural Network

The neural network was utilized to establish a relationship between the inputs and outputs of the system based on the depth of the tunnel and the cementation rate of the soil surrounding the tunnel (Tables 2 and 3). With the training received, it could consider all the desired ranges in the design. To control the training process of the neural network, a portion of the modeling was selected for testing, and another part was selected for validation. The correlation ratio between the objective functions and the outputs in the neural network program is presented in Figures 6 and 7.

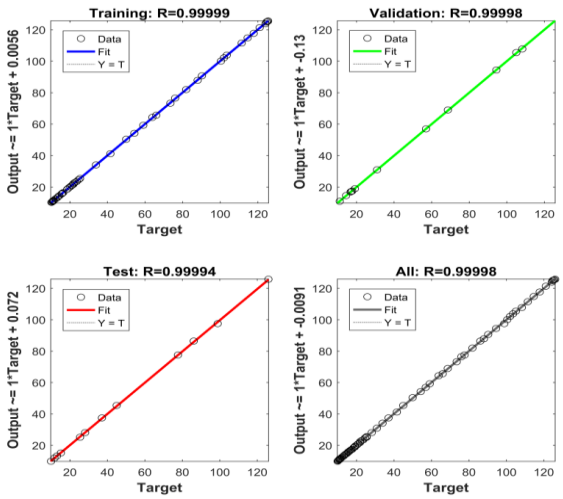

Fig 6. The Correlation ratio between the three objective functions and the output of the neural network in the depth of the tunnel

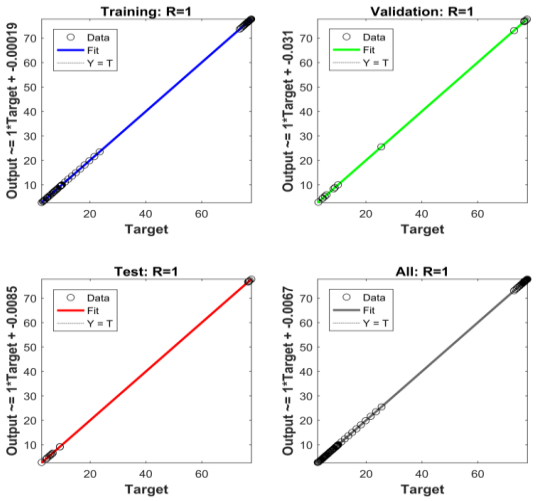

Fig 7. The Correlation ratio between the three objective functions and the neural network output in cementation rate of the soil around the tunnel

8. Results

8.1. Multi-objective Optimization using NSGA-II

After training the neural network, the modified NSGA-II algorithm was used for multi-objective optimization of the problem explained in the previous section. In these types of problems, unlike single-objective problems where there is
only one extremum point for the problem, a set of design graphs called Pareto charts is obtained based on the defined objective functions. Pareto charts optimize conflicting objective functions simultaneously. The output of these charts is a set of optimal points, and the designer chooses them based on their needs. These points do not prevail over each other.

8.2. Pareto Responses Resulting from Tunnel Depth Optimization in Liquefiable Soils

After determining the optimal tunnel depth using NSGAII, the Pareto results were presented in three dimensions, as described in Figure 8. Figures 9 and 10 were presented in two dimensions to better show the Pareto results. However, the results obtained conflict with each other in terms of the three objective functions. The reduced an objective function, such as changes in the uplift of the ground surface (f3), led to an increase in other objective functions, such as bending moment (f1) and axial force (f2) on the tunnel lining. As the objective functions f1 and f2 decrease, it also leads to the increase of the objective function f3. Therefore, it can be concluded that as one objective function decreases, one or more other objective functions in geotechnical design increase. Hence, it is crucial to find a certain point in the Pareto chart that can simultaneously optimize all the functions supposed in the design.

Based on Figure 8, points A, B, and C are essential Pareto points, and from the perspective of minimizing all objective functions in the design relative to each other, the optimal point A was chosen. Table 4 shows all the design variables and the results obtained from the objective functions related to point A, which is the most optimal location of the tunnel versus the depth in liquefiable sandy soils.

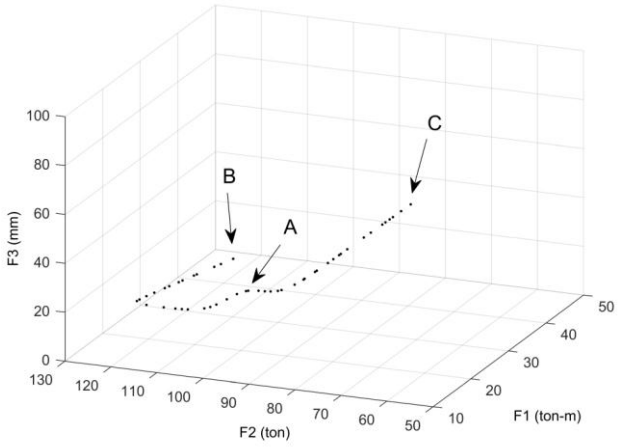

Fig 8. Pareto responses in terms of the three objective functions related to the maximum bending moment, the axial force on the tunnel lining, and the uplift of the ground surface in the liquefiable sandy soil

Table 4
Results of objective functions related to point A

Point	F1(ton-m)	F2(ton)	F3(mm)	Optimal tunnel depth (x3)
A	14.95	94.68	31.20	12.43(m)

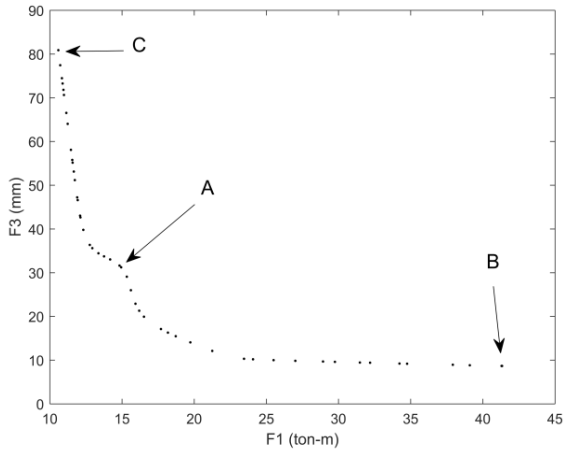

Fig 9. Pareto responses in terms of two objective functions related to the maximum bending moment applied to the tunnel lining versus the uplift of the ground

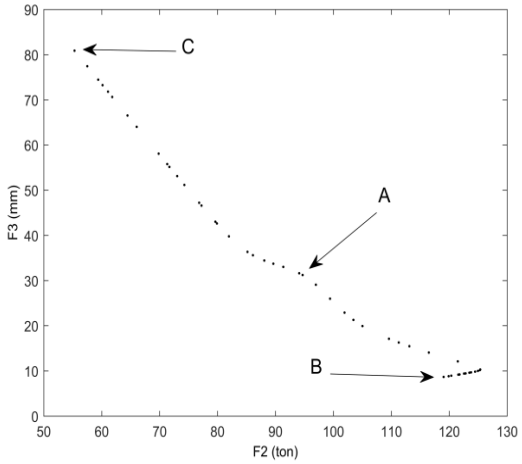

Fig 10. Pareto responses in terms of two objective functions related to the maximum axial force applied to the tunnel lining versus the uplift of the ground surface

8.3. Pareto Responses Obtained from the Optimization of the Cementation of Soil Surrounding Tunnels

The results showed that the optimum depth of the tunnel in liquefiable soils was 12.43 meters. Based on the input and output vectors presented in Table 4, multi-objective optimization of the cementation of soil surrounding the tunnels was performed using NSGAII. The Pareto responses from the perspective of the three objective functions were presented in three dimensions according to Figure 11. Figures 12 and 13 were presented in two dimensions to better show the Pareto results. However, the Pareto responses obtained from the perspective of the three objective functions conflicted with each other. As the shear force applied to the tunnel lining (f1) and the uplift of the ground surface (f2) decreases, the axial

force applied to the tunnel lining (f3) increases, and vice versa. Therefore, according to Figure 11, point D is the most optimal state from the perspective of minimizing all objective functions compared to other points such as E and F. Point D shows the most optimal the cementation rate of liquefiable soil surrounding the tunnels based on the lowest uplift of the ground surface, shear force, and axial force applied to the tunnel lining. Consequently, Table 5 was presented based on the design variables and the values obtained from the objective functions.

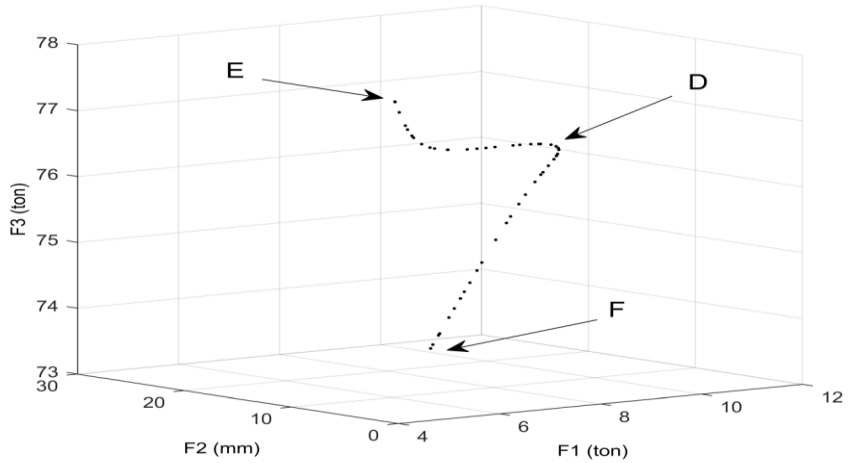

Fig 11. Pareto responses from the perspective of three objective functions related to the cementation rate of the liquefiable soil around the tunnels.

Table 5
Results of design variables related to point D

Point	F1(ton)	F2(mm)	F3(ton)	Optimal cementation (x4)
D	9.13	9.29	76.56	10.77 **(**kPa**)**

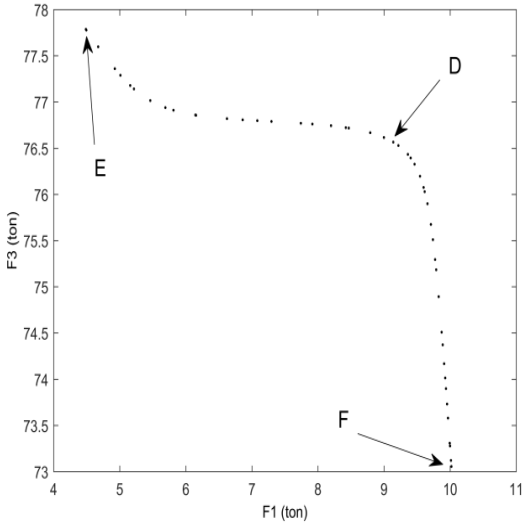

Fig 12. Pareto results pertaining to two target functions related to the maximum shear force and maximum axial force exerted on the tunnel lining

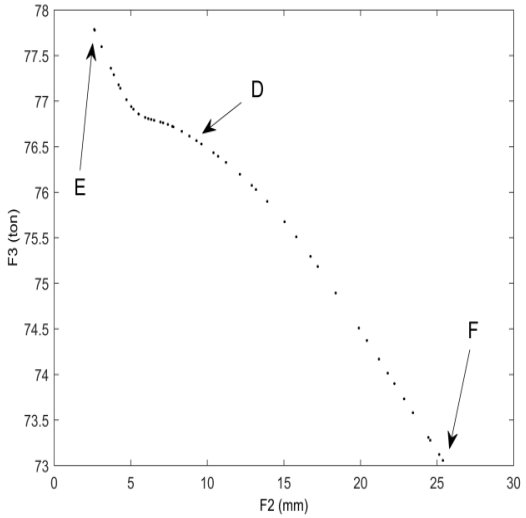

Fig 13. Pareto results pertaining to two target functions related to the uplift of the ground surface and maximum axial force exerted on the tunnel lining

9. Conclusion

The present study aimed to perform multi-objective optimization of tunnels embedded in liquefiable sandy soil. Therefore, several models were created based on changes in tunnel depth using FLAC software. The effect of these changes on the uplift of the ground surface, the maximum axial force, and the maximum bending moment applied to the tunnel lining was investigated. To reduce the damage caused by soil liquefaction, the cementation rate of the soil surrounding the tunnels was assessed. The effect of the cementation rate of the soil on the uplift of the ground surface, the maximum shear force, and the maximum axial force applied to the tunnel lining was also investigated.

Through the artificial neural network program, communication was established between the inputs and outputs of the modeling software. Based on the training received by the network, the results were obtained. This network was used as the objective function to determine the optimal values in the NSGA-II method. The general conclusions based on the analysis are as follows:

1- The soil liquefaction effects decrease by increasing the depth of the tunnel. As the depth of the tunnel increased from 8 to 20 meters in liquefied sandy soils, the uplift of the ground surface decreased by 7.8 times. However, since the overhead on the tunnel crown increased by increasing the depth, the value of the maximum bending moment and the maximum axial force on the tunnel lining increased by 1.32 and 1.3 times, respectively.

2- The soil liquefaction effects decrease by increasing the cementation rate of the soil surrounding the tunnels. As the cementation rate of athe soil surrounding the tunnels increased from 0 to 30 kPa, the uplift of the ground surface and the maximum shear force on the tunnel lining decreased by 8.8 and 1.23 times, respectively. Since increasing the cementation rate of the soil caused a decrease in the uplift of the earth's surface and the displacement of the tunnel, but an increase in the axial force on the tunnel lining, the maximum axial force on the tunnel lining increased by 6.6%.

3- The results obtained from the tunnel depth (result 1) were such that the Decreasing the uplift of the ground surface led to an increase in the bending moment and axial force on the tunnel lining, and vice versa. According to the results of the cementation rate (result 2), it can be concluded that the reduced two target functions (uplift and shear force) led to an increase in the other target function such as axial force, and vice versa. Therefore, to simultaneously optimize conflicting results, the NSGA-II optimization was used, and Pareto diagrams were obtained. Finally, based on the Pareto diagrams, can select the optimal position for the tunnel in terms of depth 12.43 m and the optimal rate of the cementation of the soil surrounding the tunnel 10.77 kPa by choosing a single point on the diagram that meets the minimum values.

References

[1] M. Azadi and S. M. M. Hosseini, "Analyses of the effect of seismic behavior of shallow tunnels in liquefiable grounds," vol. 25, no. 5, pp. 543-552, 2010.

[2] H. Liu and E. Song, "Seismic response of large underground structures in liquefiable soils subjected to horizontal and vertical earthquake excitations," vol. 32, no. 4, pp. 223-244, 2005.

[3] J.-L. Hu and H.-B. Liu, "The uplift behavior of a subway station during different degree of soil liquefaction," vol. 189, pp. 18-24, 2017.

[4] G. Zheng, W. Zhang, W. Zhang, H. Zhou, and P. Yang, "Neural network and support vector machine models for the prediction of the liquefaction-induced uplift displacement of tunnels," vol. 6, no. 2, pp. 126-133, 2021.

[5] Q. Liao, Q.-Q. Fan, and J.-J. Li, "Translation control of an immersed tunnel element using a multi-objective differential evolution algorithm," vol. 130, pp. 158-165, 2019.

[6] S. Nokande, A. Haddad, and Y. Jafarian, "Shaking Table Test on Mitigation of Liquefaction-Induced Tunnel Uplift by Helical Pile," vol. 23, no. 1, p. 04022243, 2023.

[7] A. Rashiddel, M. Abedi, D. Dias, and A. Ramesh, "Seismic analysis of segmental shallow tunnels adjacent to building foundations under soil

liquefaction and its mitigation," vol. 178, p. 108479, 2024.

[8] X.-c. ZHONG, B.-b. YI, W.-b. ZHU ,S.-r. ZHU, S.-y. LUO, and Q. WANG, "Uplift mode of shield tunnel caused by seismic liquefaction in liquefiable soil," no. 1, pp. 80-90, 2024.

[9] M. Azadi and S. M. M. Hosseini, "The uplifting behavior of shallow tunnels within the liquefiable soils under cyclic loadings," vol. 25, no. 2, pp. 158-167, 2010.

[10] H. Sharafi and P. Parsafar, "Numerical analysis of effective parameters on liquefaction occurance result from earthquake on site of buried pipelines," vol. 16, no. 3, pp. 111-120, 2016.

[11] G. W. Clough, J. Iwabuchi, N. S. Rad, and T. Kuppusamy, "Influence of cementation on liquefaction of sands, vol. 115, no. 8, pp. 1102-1117, 1989.

[12] R. Liang, X. Bai, and J. Wang, "Effect of clay particle content on liquefaction of soil, 2000, pp. 1560-1564.

[13] Z. Haiyang *et al.*, "Seismic responses of a subway station and tunnel in a slightly inclined liquefiable ground through shaking table test, vol. 116, pp. 371-385, 2019.

[14] V. Pareto and D. Cours, "Economic politique , 1896.

[15] K. Deb, A. Pratap, S. Agarwal, and T. Meyarivan, "A fast and elitist multi objective genetic algorithm: NSGA-II, vol. 6, no. 2, pp. 182-197, 2002.

[16] N. Nariman-Zadeh, K. Atashkari, A. Jamali, A. Pilechi, and X. Yao, "Inverse modelling of multi-objective thermodynamically optimized turbojet engines using GMDH-type neural networks and evolutionary algorithms," vol. 37, no. 5, pp. 437-462, .2005

[17] J. Lysmer and R. L. Kuhlemeyer, "Finite dynamic model for infinite media,", vol. 95, no. 4, pp. 859-877, 1969.

[18] F. Khoshnoudian and I. Shahrour, "Numerical analysis of the seismic behavior of tunnels constructed in liquefiable soils,", vol. 42, no. 6, pp. 1-8, 2002.

[19] M. Shabani SoltanMoradi, M. Azadi, and H. Jahanian, "Multi-objective optimisation of tunnel parameters in a liquefied sand lens under seismic loads, vol. 9, no. 4, pp. 196-210, 2022.

[20] R. Popescu and J. H. Prevost, "Comparison between VELACS numerical ‘class A’predictions and centrifuge experimental soil test results,", vol. 14, no. 2, pp. .1995 ,92-79

[21] G. R. Martin, H. B. Seed, and W. L. Finn, "Fundamentals of liquefaction under cyclic loading,", vol. 101, no. 5, pp. 423-438, 1975.

[22] S. C. Chian, K. Tokimatsu, and S. P. G. Madabhushi," Soil liquefaction–induced uplift of underground structures: physical and numerical modeling,", vol. 140, no. 10, p. 04014057, 2014.

[23] M. Alborzi, *Genetic Algorithm*, First Edition ed. Tehran: Sharif University of Technology Publishing Institute, 2009.